Journal of Inorganic Biochemistry 103 (2009) 1045–1053

Contents lists available at ScienceDirect

Journal of Inorganic Biochemistry

journal homepage: www.elsevier.com/locate/jinorgbio

Syntheses, crystal structure, spectroscopic characterization and antifungal activity of new *N*-R-sulfonyldithiocarbimate metal complexes

Leandro C. Alves [a], Mayura M.M. Rubinger [a], Renata H. Lindemann [a], Genivaldo J. Perpétuo [b], Jan Janczak [c], Liany D.L. Miranda [a], Laércio Zambolim [d], Marcelo R.L. Oliveira [a,*]

[a] Departamento de Química, Universidade Federal de Viçosa, Viçosa MG, CEP 36570-000, Brazil
[b] Departamento de Física, Instituto de Ciências Exatas e Biológicas, Universidade Federal de Ouro Preto, Ouro Preto MG, CEP 35400-000, Brazil
[c] Institute of Low Temperature and Structure Research, Polish Academy of Science, P.O. Box 1410, 50-950 Wrocław, Poland
[d] Departamento de Fitopatologia, Universidade Federal de Viçosa, Viçosa MG, CEP 36570-000, Brazil

ARTICLE INFO

Article history:
Received 19 November 2008
Received in revised form 26 March 2009
Accepted 30 April 2009
Available online 13 May 2009

Keywords:
Dithiocarbimates
Metal complexes
Crystal structures
Antifungal activity

ABSTRACT

Five new compounds with the general formula of $(Bu_4N)_2[M(RSO_2N{=}CS_2)_2]$, where Bu_4N = tetrabutylammonium cation, (M = Ni, R = 4-FC_6H_4) (**1**), (M = Zn, R = 4-FC_6H_4, 4-ClC_6H_4, 4-BrC_6H_4, 4-IC_6H_4), (**2**), (**3**), (**4**) and (**5**), respectively, were obtained by the reaction of the appropriate potassium *N*-R-sulfonyldithiocarbimate ($RSO_2N{=}CS_2K_2$) with nickel(II) chloride hexahydrate or zinc(II) acetate dihydrate in metanol:water 1:1. The elemental analyses and the IR data are consistent with the formation of the expected bis(dithiocarbimato)metal(II) complexes. The ^1H and ^{13}C NMR spectra showed the signals for the tetrabutylammonium cation and the dithiocarbimate moieties. The compounds **1**, **2** and **5** were also characterized by X-ray diffraction techniques. The nickel(II) is coordinated by two *N*-4-fluorophenylsulphonyldithiocarbimato(2-) ligands forming a planar coordination. The zinc(II) exhibits distorted tetrahedral configuration in compounds **2** and **5** due to the chelation effect of two sulfur atoms of the *N*-R-sulfonyldithiocarbimate ligands. The antifungal activities of the compounds were tested *in vitro* against *Colletotrichum gloeosporioides*, an important fungus that causes the plant disease known as anthracnose in fruit trees. All the complexes were active.

1. Introduction

Zn(II)–dithiocarbamato complexes are world-wide used in the rubber vulcanization process [1–5]. Several dithiocarbamate and *N*-substituted dithiocarbamato complexes and salts have been used as agrochemicals mainly due to their high efficiency in controlling plant fungal diseases, and relatively low toxicity [1,2,6–9]. It is interesting to note that many zinc–dithiocarbamato complexes are used simultaneously as fungicide and vulcanization accelerators. A classical example is the bis(dimethyldithiocarbamato)zinc(II) (Ziran) [2]. Zinc and nickel dithiocarbamates are also used in metal organic chemical vapour deposition (MOCVD) processes for the growth of ZnS [10–13] or NiS films [14,15].

The bis(dithiocarbimato)metal(II) complexes are necessarily anionic species. The use of anionic zinc-sulfur compounds shall provide an interesting possibility of modulation of the above mentioned applications. For example, the improvement of the antifungal activity should be possible either by the use of active counter ions, or by the variation on the solubility of the salts of the complexes due to the use of different cations.

The synthesis of a nickel(II) complex with a dithiocarbimate derived from a sulfonamide was first reported in 1989 [16]. Since then several other metal(II) complexes (including Co, Au, Zn, Pt and Pd, for example) have been described [17–22]. However, apart from $[Zn(CH_3C_6H_4SO_2N{=}CS_2)_2]^{2-}$, which was shown to be a good accelerator of vulcanization for the natural rubber [19], no other applications were described for these new compounds.

Our interest in the syntheses and characterization of dithiocarbimato metal complexes, in special dithiocarbimato ligands derived from sulfonamides, is due to their similarities with the dithiocarbamato complexes and the possibility of the sulfonyl group to improve their biological activity. Five new compounds of the general formula: $(Bu_4N)_2[M(RSO_2N{=}CS_2)_2]$ where Bu_4N = tetrabutylammonium cation, (M = Ni, R = 4-FC_6H_4) (**1**), (M = Zn, R = 4-FC_6H_4, 4-ClC_6H_4, 4-BrC_6H_4, 4-IC_6H_4), (**2**), (**3**), (**4**) and (**5**), respectively, were obtained and characterized by elemental analyses, and by IR, ^1H and ^{13}C NMR spectroscopies. The compounds **1**, **2** and **5** were also characterized by X-ray diffraction techniques.

Colletotrichum gloeosporioides is known to infect a wide variety of hosts, including vegetables, field and forage crops, fruit trees and ornamentals. For example, it is the causal agent of anthracnose, the main post-harvest disease of papaya [20]. Here we investigate the

* Corresponding author. Fax: +55 31 3899 3065.
E-mail address: marcelor@ufv.br (M.R.L. Oliveira).

0162-0134/$ - see front matter © 2009 Elsevier Inc. All rights reserved.
doi:10.1016/j.jinorgbio.2009.04.018

antifungal activities of the complexes **1**–**5** against *C. gloeosporioides* isolated from infected papaya fruits.

2. Experimental

2.1. Methods and materials

The solvents, carbon disulfide, concentrated ammonia aqueous solution and potassium hydroxide were purchased from Vetec. The *N*-4-bromophenylsulfonyl and *N*-4-iodophenylsulfonyl chlorides, 4-fluorobenzenesulfonamide, 4-chlorobenzenesulfonamide, zinc acetate dihydrate, nickel(II) chloride hexahydrate and tetrabutylammonium bromide were purchased from Alfa Aesar. The 4-bromo- and 4-iodobenzenesulfonamides were prepared by the reaction of the respective sulfonyl chlorides with concentrated ammonia aqueous solution, according to the methodology applied for the syntheses of similar compounds [23]. The *N*-R-sulfonyldithiocarbimate potassium salts dihydrate were prepared in dimethylformamide from the sulfonamides as described in the literature [24,25]. Their formations were confirmed by IR and comparison with published data [22,26,27]. These salts are soluble in water and insoluble in most of the organic solvents. Melting points were determined with a Mettler FP5 equipment. Microanalyses for C, H and N were obtained from a Perkin–Elmer 2400 CHN Elemental Analyzer. Zinc and nickel were analyzed by atomic absorption with a Hitachi Z-8200 Atomic Absorption Spectrophotometer. The IR spectra were recorded with a Perkin–Elmer 283 B infrared spectrophotometer using CsI pellets. The ^{1}H (400 MHz) and ^{13}C (100 MHz) NMR spectra were recorded with a Bruker Advance RX-400 spectrophotometer in $CDCl_3$ with TMS as internal standard. NMR abbreviations: d = doublet, m = multiplet. For the biological tests, *C. gloeosporioides* were isolated from infected papaya tissues and incubated for 10 days at 25 °C. The culture medium PDA (Potato Dextrose Agar) was purchased from Difco and was previously sterilized in autoclave for 20 min at 121 °C. Glassware and spatulas were sterilized at 140 °C for 3.5 h.

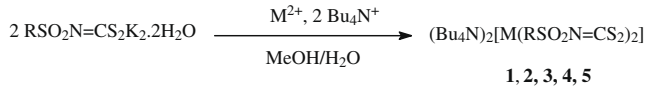

1 (M = Ni, R = FC_6H_4), **2** (M = Zn, R = FC_6H_4), **3** (M = Zn, R = ClC_6H_4)

4 (M = Zn, R = BrC_6H_4), **5** (M = Zn, R = IC_6H_4)

Scheme 1. Syntheses of **1**–**5**.

2.2. Syntheses

The syntheses of the nickel(II) and zinc(II) *N*-R-sulfonyldithiocarbimato complexes were performed as shown in the scheme 1. A mixture of nickel(II) chloride hexahydrate or zinc(II) acetate dihydrate (1.0 mmol) and tetrabutylammonium bromide (2.0 mmol) was added to a solution of the appropriated potassium *N*-R-sulfonyldithiocarbimate dihydrate (2.0 mmol) in water:methanol 1:1 (10 mL). The mixture was stirred for 1 h at room temperature. The solid obtained was filtered, washed with distilled water, ethanol, diethyl ether and dried under reduced pressure for 3 days, yielding $(Bu_4N)_2[Ni(4\text{-}FC_6H_4SO_2N{=}CS_2)_2]$ or $(Bu_4N)_2[Zn(RSO_2N{=}CS_2)_2]$ (*ca.* 70%). Single crystals of **1** (green), **2** and **5** (colourless) suitable for X-ray structure analyses were obtained after slow evaporation of the solutions of the compound **1** in methanol/water 1:1 and the compounds **2** and **5** in ethanol/chloroform 1:1.

2.2.1. Tetrabutylammonium bis(N-4-fluorophenylsulphonyldithiocarbimato)nickelate(II), $(Bu_4N)_2[Ni(4\text{-}FC_6H_4SO_2C{=}NS_2)_2]$: (*1*)

Elemental analysis: Found (calculated for $C_{46}H_{80}F_2N_4O_4S_6Ni$): C, 53.42 (53.01); H, 7.67 (7.74); N, 5.42 (5.38) and Ni, 5.48 (5.63)%. *mp* (°C): 101.3–102.2. *IR* (*most important bands*) (cm^{-1}): 1386 ν(C=N); 1281 $\nu_{as}(SO_2)$; 1143 $\nu_s(SO_2)$; 942 $\nu_{as}(CS_2)$ and 390 ν(NiS). ^{1}H NMR (δ): 7.95 (m, 4H); 7.01 (m, 4H). ^{13}C{^{1}H} NMR (δ): 211.9 (N=CS_2), 164.4 (C4, d, J_{CF} = 249 Hz), 139.8 (C1), 130.6 (C2 and C6, d, J_{CF} = 8.8 Hz), 115.1 (C3 and C5, d, J_{CF} = 22 Hz).

2.2.2. Tetrabutylammonium bis(N-4-fluorophenylsulphonyldithiocarbimato)zincate(II), $(Bu_4N)_2[Zn(4\text{-}FC_6H_4SO_2C{=}NS_2)_2]$: (*2*)

Elemental analysis: Found (calculated for $C_{46}H_{80}F_2N_4O_4S_6Zn$): C, 52.35 (52.67); H, 7.42 (7.69); N, 5.38 (5.34) and Zn, 5.97 (6.23)%. *mp* (°C): 144.2–144.6. *IR* (*most important bands*) (cm^{-1}): 1371

Table 1
Crystallographic data and structure refinement parameters.

Compound	**1**	**2**	**5**
Formula	$C_{46}H_{80}F_2N_4O_4S_6Ni$	$C_{46}H_{80}F_2N_4O_4S_6Zn$	$C_{46}H_{80}I_2N_4O_4S_6Zn$
Molecular weight	1042.21	1048.87	1264.67
Temperature (K)	295(2)	295(2)	295(2)
Crystal system	Triclinic	Monoclinic	Triclinic
Space group	P^{-1} (No. 2)	$P2_1/c$ (No. 14)	P^{-1} (No. 2)
a (Å)	9.929(3)	21.048(4)	10.309(2)
b (Å)	15.042(3)	15.197(3)	16.058(3)
c (Å)	19.654(4)	18.722(3)	18.404(4)
α (o)	100.00(2)		86.45(3)
β (°)	101.01(2)	106.49(2)	80.81(3)
γ (°)	94.38(1)		74.34(3)
V (Å^3)	2219.3(12)	5742.2(18)	2895.3(10)
Z	2	4	2
D_{calc} [g cm^{-3}]	1.228	1.213	1.451
$D_{obs.}$ [g cm^{-3}]	1.23	1.21	1.45
μ (mm^{-1})	0.614	0.693	1.748
Crystal size (mm^3)	0.420.22 × 0.12	0.28 × 0.23 × 0.23	0.28 × 0.24 × 0.12
Total/unique/observed	35,785/13,501/6978	76,060/14,914/8285	35,408/14,604/7828
Reflections (R_{int})	(0.039)	(0.071)	(0.029)
R [$F^2 > 2\sigma(F^2)$]	0.0685	0.0673	0.0392
wR [F^2 all refls][a]	0.1774	0.1813	0.0938
S	1.146	1.070	1.001
$\Delta\rho_{max}$, $\Delta\rho_{min}$ (e·Å^{-3})	+0.563, −0.331	+0.363, −0.237	+0.889, −0.616

[a] $w = 1/[\sigma^2(F_o^2) + (0.05P)^2 + 0.5P]$ for **1**, $w = 1/[\sigma^2(F_o^2) + (0.045P)^2 + 1.05P]$ for **2** and $w = 1/[\sigma^2(F_o^2) + (0.0387P)^2]$ for **5**, where $P = (F_o^2 + 2F_c^2)/3$.

ν(C=N); 1266 $\nu_{as}(SO_2)$; 1137 $\nu_s(SO_2)$; 941 $\nu_{as}(CS_2)$ and 325 ν(ZnS). ^{1}H NMR (δ): 7.93 (m, 4H), 7.00 (m, 4H). ^{13}C{^{1}H} NMR (δ): 212.0 (N=CS_2), 164.4 (C4, d, J_{CF} = 237 Hz), 139.0 (C1), 130.6 (C2 and C6, d, J_{CF} = 8.4 Hz), 115.0 (C3 and C5, d, J_{CF} = 22 Hz).

*2.2.3. Tetrabutylammonium bis(N-4-chlorophenylsulphonyl-dithiocarbimato)zincate(II), $(Bu_4N)_2[Zn(4\text{-}ClC_6H_4SO_2C{=}NS_2)_2]$: (**3**)*

Elemental analysis: Found (calculated for $C_{46}H_{80}Cl_2N_4O_4S_6Zn$): C, 50.67(51.07); H, 7.34 (7.45); N, 5.05 (5.18) and Zn, 5.94 (6.04)%. *mp* (°C): 150.0–152.3. *IR* (*most important bands*) (cm^{-1}): 1366 ν(C=N); 1265 $\nu_{as}(SO_2)$; 1135 $\nu_s(SO_2)$; 940 $\nu_{as}(CS_2)$ and 313 ν(ZnS). ^{1}H NMR (δ): 7.80 (d, 4H, J = 8.4), 7.47 (d, 4H, J = 8.4). ^{13}C{^{1}H} NMR (δ): 209.6 (N=CS_2), 141.6 (C4), 139.0 (C1), 129.6 (C2 and C6), 137.0 (C3 and C5).

*2.2.4. Tetrabutylammonium bis(N-4-bromophenylsulphonyl-dithiocarbimato)zincate(II), $(Bu_4N)_2[Zn(4\text{-}BrC_6H_4SO_2C{=}NS_2)_2]$: (**4**)*

Elemental analysis: Found (calculated for $C_{46}H_{80}Br_2N_4O_4S_6Zn$): C, 46.92(47.19); H, 6.90 (6.89); N, 4.62 (4.79) and Zn, 5.58 (5.59)%. *mp* (°C): 145.7–146.2. *IR* (*most important bands*) (cm^{-1}): 1365 ν(C=N); 1265 $\nu_{as}(SO_2)$; 1134 $\nu_s(SO_2)$; 940 $\nu_{as}(CS_2)$ and 328 ν(ZnS). ^{1}H NMR (δ): 7.80 (d, 4H, J = 8.4 Hz), 7.46 (d, 4H, J = 8.4 Hz). ^{13}C{^{1}H} NMR (δ): 209.7 (N=CS_2), 125.6 (C4), 142.1 (C1), 129.8 (C2 and C6), 131.0 (C3 and C5).

*2.2.5. Tetrabutylammonium bis(N-4-iodophenylsulphonyl-dithiocarbimato)zincate(II), $(Bu_4N)_2[Zn(4\text{-}IC_6H_4SO_2C{=}NS_2)_2]$: (**5**)*

Elemental analysis: Found (calculated for $C_{46}H_{80}I_2N_4O_4S_6Zn$): C, 43.37 (43.68); H, 6.36 (6.38); N, 4.43 (4.43) and Zn, 4.98 (5.17)%. *mp* (°C): 121.3–122.1. *IR* (*most important bands*) (cm^{-1}): 1363 ν(C=N); 1286, 1279, 1266 $\nu_{as}(SO_2)$; 1143 $\nu_s(SO_2)$; 945, 937 $\nu_{as}(CS_2)$ and 337, 313 ν(ZnS). ^{1}H NMR (δ): 7.67 (m, 8H). ^{13}C{^{1}H} NMR (δ): 209.7 (N=CS_2), 137.0 (C1), 142.7 (C3 and C5), 129.8 (C2 and C6); 98.1 (C4).

All infrared spectra showed the bands due to the vibrations of the tetrabutylammonium cation at *ca.* 2960, 2870 and 1490 cm^{-1} (most important bands). All ^{1}H NMR spectra presented the expected signals for the tetrabutylammonium cation at *ca.* δ 3.5 (CH_2N), 1.8 (CH_2), 1.4 (CH_2) and 1.0 (CH_3). The corresponding ^{13}C NMR signals were observed at *ca.* δ 59, 24, 20 and 14.

Table 2
Selected geometrical parameters (Å, °).

Compound **1**			
Ni1–S1	2.227(3)	Ni2–S4	2.147(3)
Ni1–S1	2.221(3)	Ni2–S5	2.227(3)
C1–S1	1.734(10)	C11–S4	1.756(11)
C1–S2	1.744(10)	C11–S5	1.687(10)
C1–N1	1.329(12)	C11–N2	1.297(12)
N1–S3	1.628(8)	N2–S6	1.582(9)
S3–O1	1.412(7)	S6–O11	1.434(9)
S3–O2	1.464(7)	S6–O12	1.451(9)
S3–C2	1.728(11)	S6–C12	1.781(11)
C5–F1	1.336(15)	C15–F2	1.377(14)
S1–Ni1–S2	77.7(1)	S4–Ni2–S5	79.6(1)
S1–Ni1–S2^i	102.3(1)	S4–Ni2–S5^{ii}	100.4(1)
S1–C1–S2	106.6(6)	S4–C11–S5	108.8(6)
C1–N1–S3	123.5(7)	C11–N2–S6	121.9(8)
Compound **2**			
Zn–S1	2.364(2)	Zn–S2	2.370(2)
Zn–S4	2.335(2)	Zn–S5	2.386(2)
C1–S1	1.758(4)	C1–S2	1.772(4)
C1–N1	1.293(5)	N1–S3	1.620(3)
S3–O1	1.420(3)	S3–O2	1.453(3)
S3–C2	1.749(5)	F1–C5	1.383(7)
C11–S4	1.768(5)	C11–S5	1.759(4)
C11–N11	1.273(5)	N11–S6	1.593(4)
S6–O3	1.414(3)	S6–O4	1.431(3)
S6–C12	1.764(6)	F11–C15	1.424(9)
S1–Zn–S2	77.55(5)	S4–Zn–S5	76.68(5)
S1–Zn–S4	131.39(5)	S5–Zn–S2	133.84(5)
S1–C1–S2	113.5(3)	S4–C11–S5	112.3(3)
C1–N1–S3	121.0(3)	C11–N11–S6	122.4(3)
Compound **5**			
Zn–S1	2.363(2)	Zn–S2	2.325(1)
Zn–S4	2.347(1)	Zn–S5	2.343(1)
C1–S1	1.739(3)	C1–S2	1.738(3)
C1–N1	1.318(3)	N1–S3	1.616(2)
S3–O1	1.437(2)	S3–O2	1.446(2)
S3–C2	1.766(3)	I1–C5	2.099(3)
C11–S4	1.730(3)	C11–S5	1.758(3)
C11–N2	1.304(4)	N2–S6	1.623(3)
S6–O3	1.437(3)	S6–O4	1.430(3)
S6–C12	1.771(3)	I2–C15	2.102(3)
S1–Zn–S2	77.78(4)	S4–Zn–S5	77.48(3)
S1–Zn–S4	119.85(4)	S5–Zn–S2	133.30(4)
S1–C1–S2	115.65(16)	S4–C11–S5	114.59(16)
C1–N1–S3	122.7(2)	C11–N2–S6	120.7(2)

2.3. X-ray crystallography

The single crystals of (**1**), (**2**) and (**5**) were used for data collection on a four-circle κ-geometry KUMA KM4 diffractometer equipped with two-dimensional area CCD (Charge-Coupled Device) detector. The graphite monochromatized Mo–Kα radiation (λ = 0.71073 Å) and the ω-scan technique ($\Delta\omega$ = 1°) were used for data collection. The 960 images for six different runs covering over 95% of the Ewald sphere were performed. One image was used as a standard after every 40 images for monitoring of the crystal's stability as well as for monitoring the data collection, and no correction on the relative intensity variation was necessary. Data collection and reduction along with absorption correction were performed using CrysAlis software package [28]. The max. and min. transmission factors are 0.932 and 0.786 for **1**, 0.923 and 0.8815 for **2** and 0.822 and 0.644 for **5**. The structures were solved by direct methods using SHELXS-97 giving positions of almost all non-hydrogen atoms. The remaining atoms were located from subsequent difference Fourier syntheses. The structures were refined using SHELXL-97 [29] with the anisotropic thermal displacement parameters. Hydrogen atoms of the aromatic rings were located from the difference Fourier maps, but in the final refinement the positions of all hydrogen atoms were constrained: thermal parameters and distances. Details of the data collection parameters, crystallographic data and final agreement parameters are collected in Table 1. Selected geometrical parameters are listed in Table 2. The figures were prepared using the Diamond 3.0 program [30].

2.4. Biological assay

The antifungal activity of the new compounds was evaluated by the *Poison food* technique [31] against *C. gloeosporioides.* Discs of mycelia of the fungus (diameter of 6 mm) were placed on the center of Petri dishes containing 10 mL of the culture medium (PDA) homogeneously mixed with the tested compounds **1**–**5** at the concentrations of 0.4; 0.5; 1.0; 1.5 and 2.0 mM, dimethylsulfoxide (0.1 mL), and the antibiotic chloramphenicol (Pfizer) (1000 ppm). Each treatment consisted of five repetitions and the dishes were incubated at 25 °C for 10 days. The diameter of the fungus colony was observed with the aid of a stereoscopic microscope, and measured every 24 h from the second day of incubation. The effects of the parent potassium dithiocarbimates were also tested, under the same conditions. The control (negative check treatment, five repetitions) was prepared with PDA, dimethylsulfoxide and chloramphenicol only. Tetrabutylammonium bromide (five repetitions) was inactive at the concentration of 3.0 mM.

3. Results and discussion

A molecular view of the compound **1** is illustrated in Fig. 1. The asymmetric unit of **1** consists of two tetrabutylammonium cations and two halfs of bis(*N*-4-fluorophenylsulphonyldithiocarbimato)nickelate(II) anions. The Ni atoms are S,S-chelated by two *N*-4-fluorophenylsulphonyldithiocarbimato ligands forming a planar configuration. Due to the chelating effect, the S–Ni–S angles containing the sulfur atoms of one dithiocarbimate ligand is significantly smaller than those containing the sulfur atoms from two ligands (Table 2). The crystal building is made up of discrete oppositely charged units, i.e. tetrabutylammonium cations and bis(*N*-4-fluorophenylsulphonyldithiocarbimato)nickelate(II) anions, which interact mainly by the ionic interactions

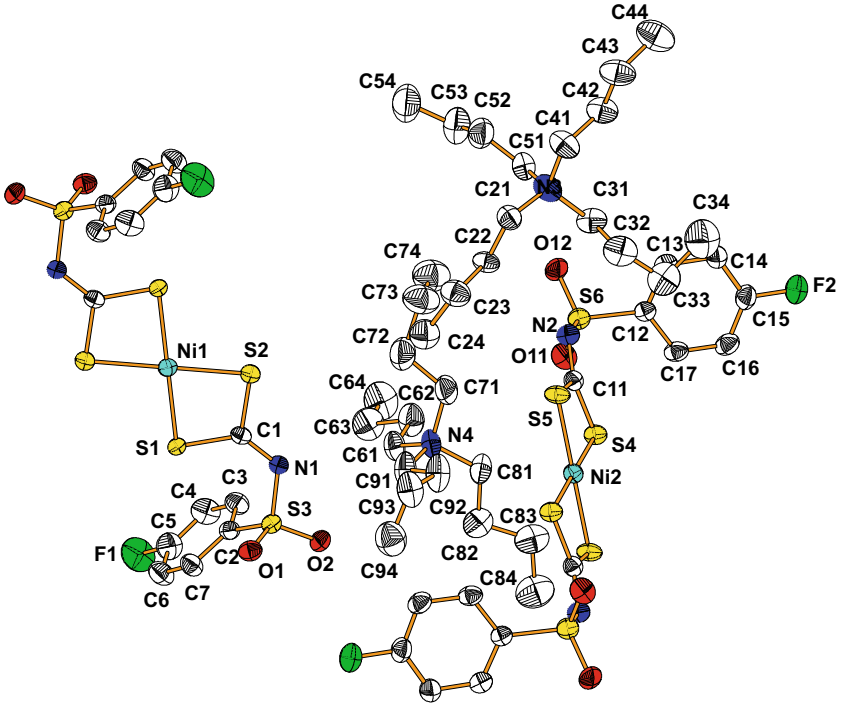

Fig. 1. View of the molecular structure of **1** with the labelling scheme and the thermal ellipsoids at the 30% probability level. Hydrogen atoms are omitted for clarity.

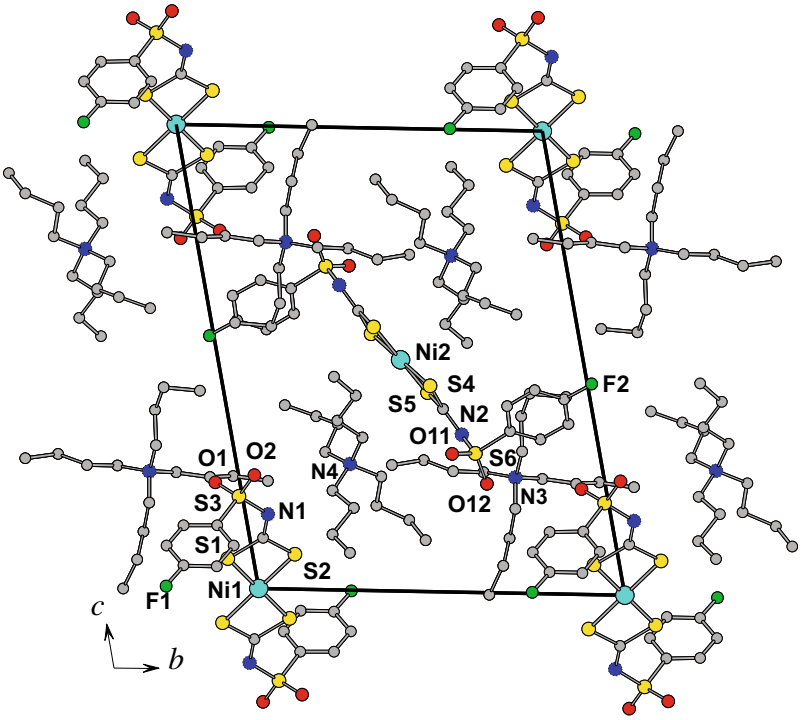

Fig. 2. Molecular arrangements of the compound **1** in the unit cells.

and by the van der Waals forces. The centrosymmetric bis(*N*-4-fluorophenylsulphonyldithiocarbimato)nickelate(II) anions containing Ni1 and Ni2 are located in the unit cell at the inversion centers of (0 0 0) and (1/2 1/2 1/2), respectively, and by translation along the *a* and *b* directions forming layers parallel to the (0 0 1) crystallographic plane. Two independent tetrabutylammonium cations form layers that are also parallel to (0 0 1) plane and are located at $z = 1/4$ and 3/4 (Fig. 2). There are no direction-specific interactions such as hydrogen bonds between the layers, but the butyl groups of the $[N(C_4H_9)_4]^+$ cations of one layer are interdigitated with the 4-fluorophenyl rings of the other layer.

The molecular structures of compounds **2** and **5** are illustrated in Figs. 3 and 5, respectively. Although the compounds **2** and **5** are different only at the ring substituents (F in **2** and I in **5**) the complexes are not isostructural. Compound **2** crystallises in the monoclinic space group while compound **5** crystallises in the triclinic group. However, the zinc(II) in both compounds exhibits similar coordination environment. The Zn atom coordinates via the two sulfur atoms of each dithiocarbimate group in **2** and **5**, forming a distorted tetrahedral coordination. The Zn–S bond lengths are comparable in both compounds (Table 2). As in compound 1, the S–M–S angles containing the sulfur atoms of one dithiocarbimate ligand in **2** and **5** are significantly smaller than

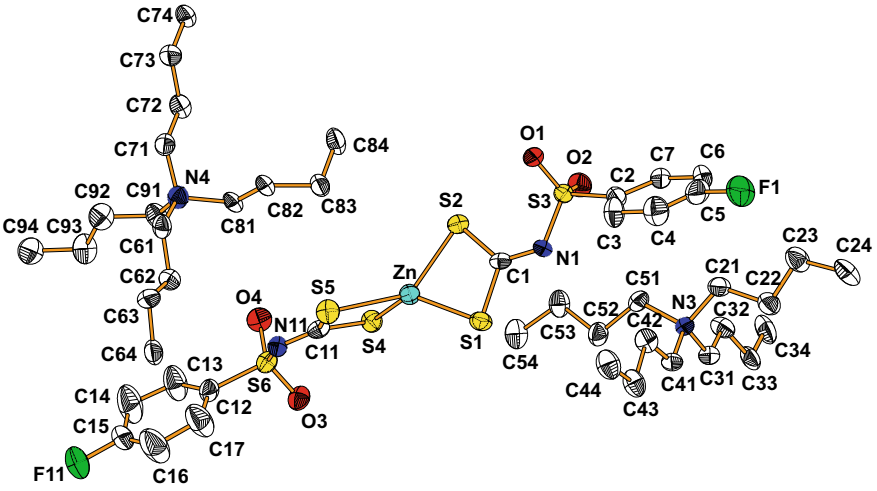

Fig. 3. View of the molecular structure of **2** with labelling of the atoms and the thermal ellipsoids at the 30% probability level. Hydrogen atoms are omitted for clarity.

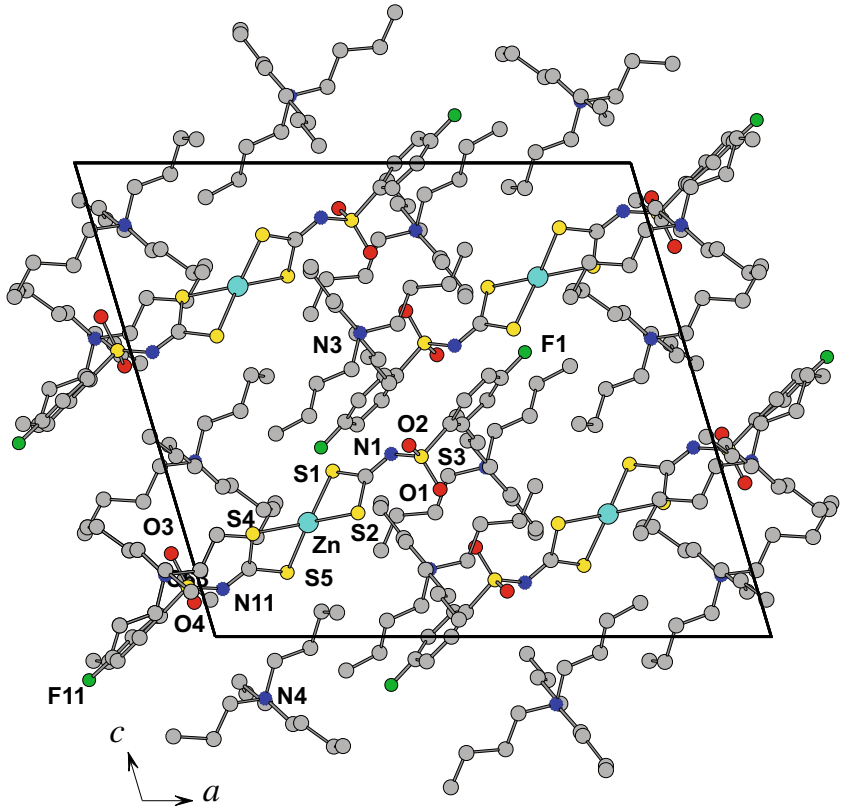

Fig. 4. Molecular arrangements of the compound **2** in the unit cells.

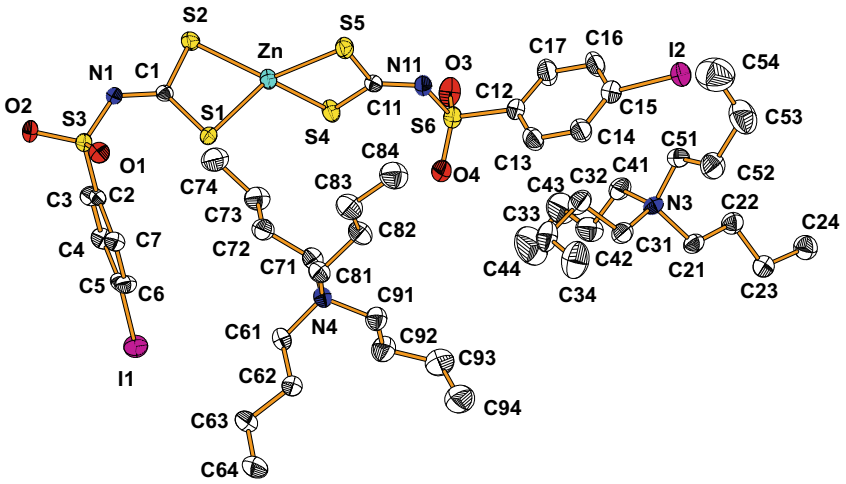

Fig. 5. View of the molecular structure of **5** with the labelling of the atoms and the thermal ellipsoids at the 30% probability level. Hydrogen atoms are omitted for clarity.

Table 3
Comparison of the conformation of tetrabutylammonium cation carbon chains in the crystals of **2** and **5**.

Torsion angle	2	5
C21–C22–C23–C24	−175.9(4)	−175.6(3)
C31–C32–C33–C34	−176.5(4)	63.9(4)
C41–C42–C43–C44	−179.6(4)	179.0(4)
C51–C52–C53–C54	−175.7(4)	67.8(4)
C61–C62–C63–C64	177.8(4)	176.1(3)
C71–C72–C73–C74	179.6(4)	−167.0(3)
C81–C82–C83–C84	83.0(4)	168.6(3)
C91–C92–C93–C94	−178.1(4)	67.9(4)

those containing the sulfur atoms of two ligands (Table 2). The geometries of the whole Zn-bis(dithiocarbimato) anions in **2** and in **5** are different. In **2** the $[Zn(FC_6H_4SO_2NCS_2)_2]^{2-}$ anion adopts an almost linear conformation. The torsion angles of C1–N1–S3–C2 and C11–N11–S6–C12 describing the conformation of the ligands are almost equal: 173.7(2)° and 172.0(2)°, respectively. This is in contrast to the conformation of the $[Zn(IC_6H_4SO_2NCS_2)_2]^{2-}$ anion in **5**, in which the respective angles are −68.2(2)° (C1–N1–S3–C2) and −175.4(2)° (C11–N11–S6–C12). Thus in **5** one of the two phenyl rings is turned by ∼100° in relation to that in **2**. Different conformations of Zn-dithiocarbimato anions in **2** and in **5** imply different conformations of the carbon chains of the tetrabuthylammonium cations (Table 3). In their crystals the molecular arrangements are mainly determined by the electrostatic interactions between the oppositely charged units and by the van der Waals forces. In both structures there are no observed hydrogen bonds (Figs. 4 and 6).

The compounds **1**–**5** are stable at the ambient conditions. The compound **1** is insoluble in water and soluble in most of the organic solvents. The zinc compounds **2**–**5** are slightly soluble in water, methanol and ethanol, and are soluble in chloroform and dichloromethane.

There is a strong band in the 1300–1400 cm^{-1} region in the IR spectra of the compounds. This band is in the same region of the spectra of other metal(II)–dithiocarbimato complexes [22,26,27], and was assigned to νCN band vibration of the $RSO_2N{=}CS_2$ group.

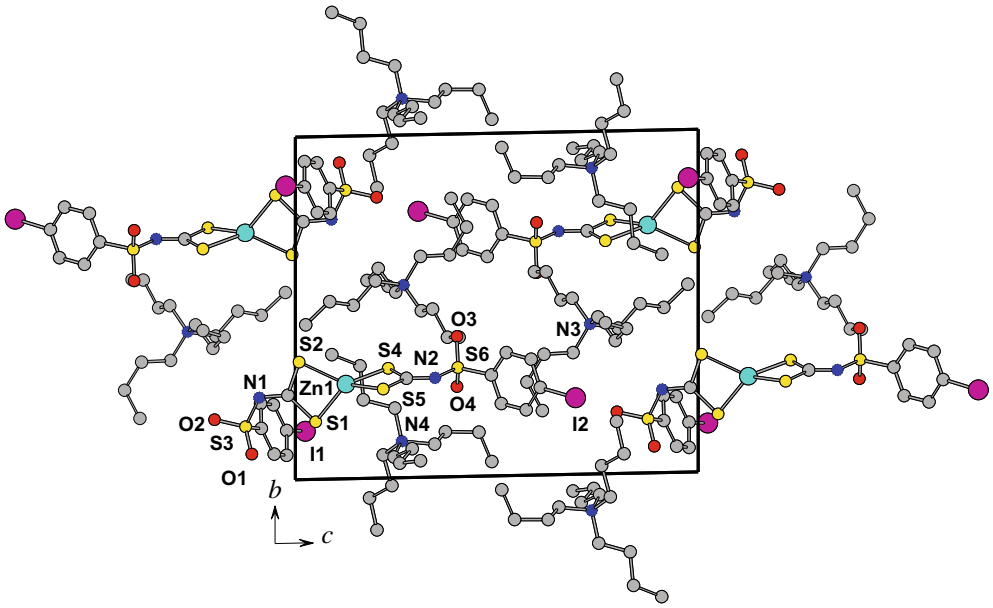

Fig. 6. Molecular arrangements of the compound **5** in the unit cells.

They are shifted to higher wavenumbers with respect to the spectra of the ligands [22,26,27]. The spectral region of 1000–900 cm^{-1} is characteristic for the disulfuric chelation [32]. A medium band at *ca.* 940 cm^{-1} was observed in the spectra of all compounds. This band is assigned to the $\nu_{as}CS_2$ and is shifted to lower wavenumbers with respect to the spectra of the ligands [22,26,27]. The positions observed for the $\nu_{as}CS_2$ and νCN bands in the spectra of the compounds here studied are consistent with the complexation of the dithiocarbimate group by two sulfur atoms [26], and with the increased importance of the canonical form (c) after complexation (Scheme 2). The spectra of the compounds also show the expected band of medium intensity in the 300–400 cm^{-1} range assigned to the M–S stretching vibration indicating the chelation by two sulfur atoms [33].

The NMR spectra showed the expected signals for the compounds. The ^1H and ^{13}C spectra of the compound **1** are typical for diamagnetic species, consistent with a square plane geometry for the fragment NiS_4. The ^1H NMR spectra of all the compounds showed the signals for the hydrogen atoms of the tetrabutylammonium cation. The remaining signals could be assigned to the aromatic moiety. The integration curves on the ^1H NMR spectra were consistent with a 2:1 proportion between the tetrabutylammonium cation and the metal(II)–dithiocarbimato complexes. The ^{13}C NMR spectra showed the expected signals for the tetrabutylammonium cation and the pertinent carbon atoms in the complexes anions. The spectroscopic data are in agreement with the single crystal X-ray analyses (Table 4).

Anthracnose, caused by *C. gloeosporioides*, is a major post-harvest disease in many fruits such as citrus, mango, papaya and grapes. The control of fungal diseases on plants often requires the use of fungicides and there is a continuous need for new classes of antifungal agents due to the development of resistant strains. Compounds **1**–**5** were able to inhibit the growth of *C. gloeosporioides* in the *in vitro* test *Poison Food*. The lack of activity of tetrabutylammonium bromide even at a higher concentration (3 mM) indicated that the activity presented by the new compounds **1**–**5** was due to the complex anions. To the best of our knowledge these results are the first confirmation of antifungal activities of metal–sulfonyldithiocarbimato complexes.

Fig. 7 shows the colony growth of *C. gloeosporioides* (diameter of the colony halo) over the 10 days of incubation at 25 °C (control) in

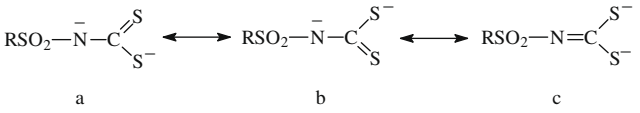

Scheme 2. Three canonical forms for the *N*-R-sulfonyldithiocarbimate anion.

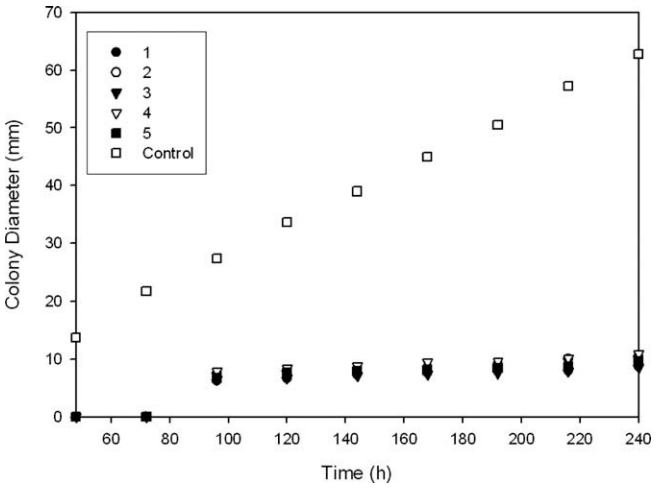

Fig. 7. Colony diameter of *C. gloeosporioides* over the 10 days of incubation at 25 °C when treated with compounds **1**–**5** (at 2 mmol L^{-1}) in comparison with the control (100% growth).

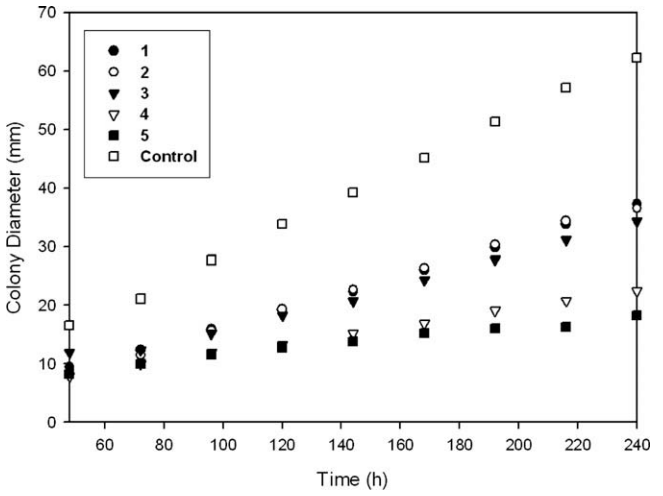

Fig. 8. Colony diameter of *C. gloeosporioides* over the 10 days of incubation at 25 °C when treated with compounds **1**–**5** (at 1 mmol L^{-1}) in comparison with the control (100% growth).

comparison with the growth in the presence of compounds **1**–**5** at 2 mM. It is interesting to note that, in the presence of compounds **1**–**5**, some growth could only be noted on the fourth day of incubation, while it was quite visible from the second day on the control

Table 4
Comparison between crystallographic and spectroscopic data for the CN bond in the dithiocarbimate anions.

Compounds	νCN (cm^{-1})	^{13}C NMR (NCS_2) (ppm)	CN length (Å)
4-$FC_6H_4SO_2N{=}CS_2K_2.2H_2O$[a]	1259	225.3	1.351(2)
$[Ni(4\text{-}FC_6H_4SO_2N{=}CS_2)_2]^{2-}$ (**1**)	1386	211.9	1.329(12), 1.297(12)
$[Zn(4\text{-}FC_6H_4SO_2N{=}CS_2)_2]^{2-}$ (**2**)	1371	212.0	1.293(5)
4-$ClC_6H_4SO_2N{=}CS_2K_2.2H_2O$[b,c]	1261	225.0	1.354(5)
$[Zn(4\text{-}ClC_6H_4SO_2N{=}CS_2)_2]^{2-}$ (**3**)	1366	209.6	–
4-$BrC_6H_4SO_2N{=}CS_2K_2.2H_2O$[c]	1259	225.5	–
$[Zn(4\text{-}BrC_6H_4SO_2N{=}CS_2)_2]^{2-}$ (**4**)	1365	209.7	–
4-$IC_6H_4SO_2N{=}CS_2K_2.2H_2O$[d]	1280	223.9	–
$[Zn(4\text{-}IC_6H_5SO_2N{=}CS_2)_2]^{2-}$ (**5**)	1363	209.7	1.318(3)

[a] Ref. [27].
[b] Ref. [25].
[c] Ref. [22].
[d] Ref. [26].

Table 5
Inhibition of *C. gloeosporioides* growth by the complexes **2**–**5** at different concentrations on the 10th day of incubation at 25 °C, and IC_{50} (mM) of the complexes.

Substances	Inhibition (%), concentration (mM)					IC_{50}
	0.4	0.5	1.0	1.5	2.0	
$(Bu_4N)_2[Zn(4\text{-}FC_6H_4SO_2N{=}CS_2)_2]$ (**2**)	7.9	21.5	41.4	61.5	86.0	1.2
$(Bu_4N)_2[Zn(4\text{-}ClC_6H_4SO_2N{=}CS_2)_2]$ (**3**)	9.6	24.4	44.9	68.4	86.5	1.2
$(Bu_4N)_2[Zn(4\text{-}BrC_6H_4SO_2N{=}CS_2)_2]$ (**4**)	19.2	31.9	64.0	75.5	82.6	0.96
$(Bu_4N)_2[Zn(4\text{-}IC_6H_5SO_2N{=}CS_2)_2]$ (**5**)	38.2	46.9	70.6	73.3	84.6	0.61

Petri dishes. From the fourth day up to the end of the experiment the growth was negligible for the five treatments, while *C. gloeosporioides* continued to develop linearly in the control dishes. At this concentration, there were no significant differences in the activity of the new compounds, but at lower concentrations, the increase on the size of the halide substituent from fluorine to bromine, and especially to iodine substantially increased the activity of the metal complex (Fig. 8). The increase in the lipophilicity from the complex **2** to **5** might enable stronger interactions with the cellular walls.

Table 5 shows the inhibition percentage of the fungus colony on the 10th day of incubation at the different concentrations tested for compounds **2**–**5**. The concentrations of the compounds to inhibit 50% of the colony growth (IC_{50}) were calculated from the equations obtained from the dose–response curves. Compound **5** was the most active, showing approximately half the IC_{50} dose when compared to compounds **2** and **3**, with fluorine and chlorine substituents. The same methodology was applied to compound **1**, but at higher concentrations it could be noted that the mixtures on the Petri dishes were not completely homogeneous, due to the much smaller solubility of compound **1** in the medium, when compared to the zinc complexes. Due to this low solubility, the dose–response curve for compound **1** was not linear enough to enable a precise calculation of its IC_{50}. However, it seems to be as active as the analogous zinc complex **2**.

Differently from their metal complexes, the potassium dithiocarbimates ($RSO_2N{=}CS_2K_2{\cdot}2H_2O$) are not very stable under the ambient conditions. Their solutions show white solid deposits on standing at the room temperature for a few days, and when kept in the solid state at ambient temperature, these potassium salts are also converted in white solids after several months [26]. Consequently, although the potassium dithiocarbimate were also active, the complexation with metals such as zinc or nickel seems to be important to give the necessary stability in order to allow any future applications in the control of pathogenic fungi. Furthermore, the potassium dithiocarbimate would show less applicability, especially in field crops, as water soluble fungicides are easily leached out.

Probably due to their instability, the dose–response curves were not always linear for the potassium dithiocarbimates, and the data were not satisfactorily reproducible when the tests were repeated in different days. So, the IC_{50} were not calculated for these salts, but it can be pointed out that in almost all concentrations the potassium salts were less active than the corresponding complexes. For example, at 0.4, 1.0 and 1.5 mM, $4\text{-}IC_6H_4SO_2N{=}CS_2K_2$ inhibited *C. gloeosporioides* mycelial growth in approximately 15%, 45% and 65% while the compound **5** inhibited in 38.2%, 70.6% and 84.6%, respectively. Different methodologies are necessary for a more precise evaluation of the activity of the potassium dithiocarbimates and of the less soluble nickel complexes. These studies will be carried out in due course.

4. Conclusion

New nickel(II) (**1**) and zinc(II) (**2**–**5**) anionic bis(dithiocarbimato) complexes were obtained as tetrabutylammonium salts. The complexes were isolated and characterized by elemental analyses, IR, ^1H and ^{13}C NMR. The **1**, **2** and **5** complexes were analyzed by single crystal X-ray diffraction techniques. The wavenumbers of the IR $\nu C{=}N$ vibration observed in the spectra of the compounds are greater than that observed for the free ligands. The NMR spectra are in agreement with the suggestion that upon complexation the double character of the CN bond increases [22,26,27]. This fact is in accordance with an increase of the contribution of the canonical form (c) (Scheme 2) to the resonance hybrid from the free ligands to the metal complexes. This suggestion is supported by the single crystal X-ray analysis. All the new substances were active against *C. gloeosporioides*. Larger substituents on the aromatic ring enhance their activity, which is due to the anionic complex only. Changing the cation by other counter ion might enhance the activity of these new fungicides, either by improving their physicochemical properties, or by adding a new mode of action (in the case of the use of an active cation). Further studies are being carried out in order to determine their mode of action and to modulate their activities. Their application in the control of other fungal classes, including plant and human pathogenic fungi and mould growth on various surfaces, shall be investigated.

Acknowledgements

This work has been supported by CNPq, CAPES and FAPEMIG (Brazil).

Appendix A. Supplementary material

Crystallographic data for the structural analysis have been deposited with the Cambridge Crystallographic Data Centre, CCDC 702964, 702965 and 702966 for **1**, 2 and **5**, respectively. These data can be obtained free of charge at http://www.ccdc.cam.ac.uk or from the Cambridge Crystallographic Data Centre, 12, Union Road, Cambridge CB2 1EZ, UK; fax: +44 1223/336 033; e-mail: deposit@ccdc.cam.ac.uk. Supplementary data associated with this article can be found, in the online version, at doi:10.1016/j.jinorgbio.2009.04.018.

References

[1] D. Coucouvanis, Prog. Inorg. Chem. 11 (1969) 233–371.
[2] D. Hogarth, Prog. Inorg. Chem. 53 (2005) 71–561.
[3] L. Bateman, C.G. Moore, M. Porter, B. Saville, The Chemistry and Physics of Rubber-like Substances, Maclaren & Sons Ltd., London, 1963.
[4] P.J. Nieuwenhuizen, S. Timal, J.G. Haasnoot, A.L. Spek, J. Reedijk, Chem. Eur. J. 3 (1997) 1846–1851.
[5] P.J. Nieuwenhuizen, A.W. Ehlers, J.G. Haasnoot, S.R. Janse, J. Reedijk, E.J. Baerends, J. Am. Chem. Soc. 121 (1999) 163–168.
[6] M.J. Burkitt, H.S. Bishop, L. Milne, S.Y. Tsang, G.J. Provan, C.S.I. Nobel, S. Orrenius, A.F.G. Slater, Arch. Biochem. Biophys. 353 (1998) 73–84.
[7] A.K. Malik, W. Faubel, Pestic. Sci. 55 (1999) 965–970.
[8] E. Humeres, N.A. Debacher, M.M.S. Sierra, J. Org. Chem. 64 (1999) 1807–1813.
[9] T. Kamenosono, H. Shimada, T. Funakoshi, S. Kojima, Toxicology 170 (2002) 103–110.
[10] M. Motevalli, P. O'Brien, J.R. Walsh, I.M. Watson, Polyhedron 15 (1996) 2801–2808.
[11] D.M. Frigo, O.F.Z. Khan, P. O'Brien, J. Cryst. Growth 96 (1989) 989–992.
[12] B.L. Druz, A.I. Dyadenko, Yu.N. Evtukhov, M.Ya. Rakhlin, A.E. Rodionov, Inorg. Mater. 26 (1990) 24–26.

[13] R.D. Pike, H. Cui, R. Kershaw, K. Dwight, A. Wold, T.N. Blanton, A.A. Wernburg, H.J. Gysling, Thin Solid Films 224 (1993) 221–226.
[14] R. Nomura, H. Hayata, Trans. Mater. Res. Soc. Jpn. 26 (2001) 1283–1286.
[15] P. O'Brien, J.H. Park, J. Waters, Thin Solid Films 431 (2003) 502–505.
[16] H.U. Hummel, U. Korn, Z. Naturforsch. 44B (1989) 29–34.
[17] M.R.L. Oliveira, V.M. De Bellis, Trans. Metal. Chem. 24 (1999) 127–130.
[18] R.S. Amim, M.R.L. Oliveira, J. Amim Jr., Trans. Metal Chem. 31 (2006) 1071–1074.
[19] R.M. Mariano, M.R.L. Oliveira, M.M.M. Rubinger, L.L.Y. Visconte, Eur. Polym. J. 43 (2007) 4706–4711.
[20] F.L. Palhano, T.T.B. Vilches, R.B. Santos, M.T.D. Orlando, J.A. Ventura, P.M.B. Fernandes, Int. J. Food Microbiol. 15 (2004) 61–66.
[21] R.S. Amim, M.R.L. Oliveira, G.J. Perpétuo, J. Janczak, L.D.L. Miranda, M.M.M. Rubinger, Polyhedron 27 (2008) 1891–1897.
[22] M.R.L. Oliveira, V.M. De Bellis, Trans. Metal. Chem. 24 (1999) 127–130.
[23] A.I. Vogel, A Textbook of Practical Organic Chemistry Including Qualitative Organic Analysis, Longmans, London, 1956.
[24] K. Hartke, Archiv der Pharmazie 299 (1966) 174–178.
[25] H.U. Hummel, U. Korn, Z. Naturforsch. 44B (1989) 24–28.
[26] E.F. Franca, M.R.L. Oliveira, S. Guilardi, R.P. Andrade, R.H. Lindemann, J. Amim Jr., J. Ellena, V.M. De Bellis, M.M.M. Rubinger, Polyhedron 25 (2006) 2119–2126.
[27] R.S. Amim, M.R.L. Oliveira, G.J. Perpétuo, J. Janczak, L.D.L. Miranda, M.M.M. Rubinger, Polyhedron 27 (2008) 1891–1897.
[28] Oxford Diffraction Poland (2006). CrysAlis CCD and CrysAlis Red, Version 171.32.6, Wrocław, Poland.
[29] G.M. Sheldrick, *SHELXS*-97 and *SHELXL*-97, Programs for the Solution and Refinement of Crystal Structures, University of Göttingen, Göttingen, Germany, 1997.
[30] K. Brandenburg, H. Putz, Diamond 3.0. Crystal and Molecular Structure Visualization, University of Bonn, Germany, 2006.
[31] G. Singh, P. Marimuthu, C.S. Heluani, C.A.N. Catalan, J. Agri. Food Chem. 54 (2006) 174–181.
[32] D.A. Brown, W.K. Glass, M.A. Burke, Spectrochim. Acta A32 (1976) 137–143.
[33] K. Nakamoto, Infrared and Raman of Inorganic and Coordination Compounds, John Wiley & Sons, Inc., New York, 1978.